Earth and Planetary Science Letters 486 (2018) 1–14

Contents lists available at ScienceDirect

Earth and Planetary Science Letters

www.elsevier.com/locate/epsl

When does eruption run-up begin? Multidisciplinary insight from the 1999 eruption of Shishaldin volcano

Daniel J. Rasmussen[a,*], Terry A. Plank[a], Diana C. Roman[b], John A. Power[c], Robert J. Bodnar[d], Erik H. Hauri[b]

[a] Lamont-Doherty Earth Observatory, Columbia University, 61 Route 9W, PO Box 1000, Palisades, NY, 10964, USA
[b] Department of Terrestrial Magnetism, Carnegie Institution for Science, 5241 Broad Branch Road, N.W., Washington, D.C., 20015, USA
[c] Alaska Volcano Observatory, US Geological Survey, Volcano Science Center, 4200 University Dr., Anchorage, AK, 99508, USA
[d] Department of Geosciences, Virginia Tech, 4044 Derring Hall, 926 West Campus Drive, Virginia Tech, Blacksburg, VA, 24061, USA

A R T I C L E I N F O

Article history:
Received 15 September 2017
Received in revised form 20 December 2017
Accepted 2 January 2018
Available online xxxx
Editor: T.A. Mather

Keywords:
run-up
precursor
eruption
diffusion chronometry
magma mixing
shear-wave splitting

A B S T R A C T

During the run-up to eruption, volcanoes often show geophysically detectable signs of unrest. However, there are long-standing challenges in interpreting the signals and evaluating the likelihood of eruption, especially during the early stages of volcanic unrest. Considerable insight can be gained from combined geochemical and geophysical studies. Here we take such an approach to better understand the beginning of eruption run-up, viewed through the lens of the 1999 sub-Plinian basaltic eruption of Shishaldin volcano, Alaska. The eruption is of interest due to its lack of observed deformation and its apparent long run-up time (9 months), following a deep long-period earthquake swarm. We evaluate the nature and timing of recharge by examining the composition of 138 olivine macrocrysts and 53 olivine-hosted melt inclusions and through shear-wave splitting analysis of regional earthquakes. Magma mixing is recorded in three crystal populations: a dominant population of evolved olivines (Fo_{60-69}) that are mostly reversely zoned, an intermediate population (Fo_{69-76}) with mixed zonation, and a small population of normally zoned more primitive olivines (Fo_{76-80}). Mixing-to-eruption timescales are obtained through modeling of Fe–Mg interdiffusion in 78 olivines. The large number of resultant timescales provides a thorough record of mixing, demonstrating at least three mixing events: a minor event ∼11 months prior to eruption, overlapping within uncertainty with the onset of deep long-period seismicity; a major event ∼50 days before eruption, coincident with a large (M5.2) shallow earthquake; and a final event about a week prior to eruption. Shear-wave splitting analysis shows a change in the orientation of the local stress field about a month after the deep long-period swarm and around the time of the M5.2 event. Earthquake depths and vapor saturation pressures of Raman-reconstructed melt inclusions indicate that the recharge magma originated from depths of at least 20 km, and that mixing with a shallow magma or olivine cumulates occurred in or just below the edifice (<3 km depth). Deformation was likely outside the spatial and temporal resolution of the satellite measurements. Prior to eruption magma was stored over a large range of depths (∼0–2.5 km below the summit), suggesting a shallow, vertical reservoir that could provide another explanation for the lack of detectable deformation. The earliest sign of unrest (deep long-period seismicity) coincides temporally with magmatic activity (magma mixing and a change in the local stress state), possibly indicating the beginning of eruption run-up. The more immediate run-up began with the major recharge event ∼50 days prior to eruption, after which the signs of unrest became continuous. This timescale is long compared to the seismic run-up to other basaltic eruptions (typically hours to days). Other volcanoes classified as open-system, based on their lack of precursory deformation, also tend to have relatively long run-up durations, which may be related to the time required to fill the shallow reservoir with magmas sourced from greater depth.

1. Introduction

Unraveling the sequence and duration of magmatic events preceding volcanic eruptions is central to understanding volcanoes and the hazards they pose. Real-time volcano monitoring during

* Corresponding author.
E-mail addresses: danielr@ldeo.columbia.edu (D.J. Rasmussen), tplank@ldeo.columbia.edu (T.A. Plank), droman@carnegiescience.edu (D.C. Roman), jpower@usgs.gov (J.A. Power), rjb@vt.edu (R.J. Bodnar), ehauri@carnegiescience.edu (E.H. Hauri).

https://doi.org/10.1016/j.epsl.2018.01.001
0012-821X/

unrest provides unparalleled insight into stirrings deep within a magmatic system (Sparks, 2003). However, translation of the signals into magmatic processes is challenging, and only a handful of eruptions are well monitored. Petrology offers powerful tools to study eruption run-up that benefit from direct response to magmatic forcings and applicability to most eruptions. Diffusion chronometers (or crystal clocks) give insight into crystal residence times (Cooper and Kent, 2014), mixing-to-eruption timescales (Costa and Chakraborty, 2004), magma ascent rates (Lloyd et al., 2013), and cooling rates (Newcombe et al., 2014). Solubility barometers indicate the depths of magmatic processes (Spilliaert et al., 2006). Further insight into the timing of magmatic events can be gained by applying modern seismological techniques to older datasets to glean new information (e.g., stress field analysis; Roman and Gardine, 2013). Developing these tools, and tying them to monitoring data, will help identify eruption triggers and understand the significance of real-time observations during unrest (e.g., Kahl et al., 2011; Rae et al., 2016).

An important goal for combined geochemical and geophysical research is understanding the earliest signals of volcanic unrest. In many cases, magma recharge and mixing are thought to initiate eruptions (Sparks et al., 1977). Geodetic methods can give insight into the first signs of recharge (Lu and Dzurisin, 2014). However, many volcanoes lack measurable deformation signals (open-system volcanoes) for reasons that are not well understood (Ebmeier et al., 2013). Deep long-period earthquakes (DLPs) may result from magma movement deep within the crust (Power et al., 2004), thereby providing another potential early sign of recharge. Interestingly, there have only been a few cases where DLPs have been identified as part of a precursory sequence (e.g., Power et al., 2013, 2004; White, 1996). To better understand the duration of eruption run-up, it is necessary to combine information on magma recharge with extremely subtle indicators of stress or deformation (e.g., shear-wave splitting) and the occurrence of DLPs prior to eruptions.

As a case study, we examine the 1999 sub-Plinian basaltic eruption of Shishaldin volcano, Alaska, one of the few examples where DLPs are suggested to be the earliest precursor to eruption (Power et al., 2004). While most basaltic eruptions have run-up durations on the order of hours to days (Passarelli and Brodsky, 2012), the earliest detected DLP swarm at Shishaldin occurred ∼9 months prior to eruption, implying an abnormally long run-up. Interferometric synthetic aperture radar (InSAR) images that span the DLP swarm lack indication of inflation (Moran et al., 2006), which may be related to spatiotemporal limitations of the old dataset and/or the general lack of observed inter- and intra-eruptive deformation at Shishaldin over the past 20 yrs (Lu and Dzurisin, 2014; Moran et al., 2006). We focus on this eruption to determine (1) when eruption run-up began and (2) why there was no readily InSAR-detectable geodetic signal. Both require a detailed understanding of the location of magmas in space and time prior to the eruption. A comprehensive set of real-time observations chronicle the run-up and ultimate VEI 3 eruption (Nye et al., 2002). We build on these observations using geochemical and geophysical tools. Magma depths are examined by employing solubility barometry, using measured and reconstructed volatile contents of melt inclusions. The timing of magma recharge is investigated using compositional gradients in olivine for diffusion chronometry and seismic shear-wave splitting patterns as indicators of stress. Finally, we consider Shishaldin in the context of other open-system volcanoes and compare our results with seismically defined run-up timescales from the literature (Passarelli and Brodsky, 2012).

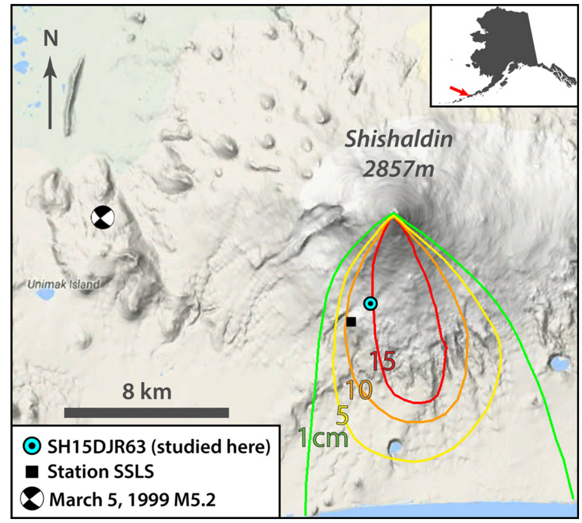

Fig. 1. Thickness of deposits from the 1999 eruption of Shishaldin volcano (after Stelling et al., 2002). The total volume of erupted products is 4.3×10^7 m^3 (or 1.4×10^7 m^3 dense rock equivalent; Stelling et al., 2002). Sample SH15DJR63 (IGSN: TAP00005C), located at N54.71895 W163.98648 (WGS84), was collected in 2015 and is studied here. SSLS is a three-component short-period seismic station operated by the Alaska Volcano Observatory. Focal mechanism for the M5.2 from Moran et al. (2002). Base map from Google Maps.

2. Eruption timeline

Activity precursory to the 1999 eruption of Shishaldin likely started in July 1998 with the occurrence of a swarm of long period (LP) earthquakes, spanning depths of >15 to ∼0 km below sea level (BSL) (Moran et al., 2002). A second, minor swarm occurred in September–October (Moran et al., 2002). Little activity followed until February 1999, when low-level seismic tremor initiated (Thompson et al., 2002). On February 9, a thermal anomaly appeared in the summit crater (Dehn et al., 2002). Around the same time, vigorous steam plumes were observed, and low-level tremor became continuous (Nye et al., 2002). Precursory activity reached a crescendo on March 4 with a shallow (∼0 km BSL), strike-slip M5.2 tectonic earthquake located 16 km west of Shishaldin (Moran et al., 2002). Aftershocks followed, causing a significant increase in the rate of earthquakes (Thompson et al., 2002). After minor Strombolian activity that began as early as late March (Dehn et al., 2002), a sub-Plinian, VEI 3 event occurred on April 19. In only ∼80 mins, $\sim 4.3 \times 10^7$ m^3 of basaltic scoria (or 1.4×10^7 km^3 dense rock equivalent) was ejected in two short bursts, with plumes reaching heights of ∼9 and ∼16 km (Nye et al., 2002). After the initial sub-Plinian explosion, the eruption shifted to vigorous, pulsating Strombolian bursts for ∼2.5 hrs, and similar activity continued sporadically into May (Nye et al., 2002).

3. Sample description

We study a tephra fall deposit (SH15DJR63; IGSN: TAP00005C; Fig. 1) associated with the sub-Plinian phase of the eruption, the only phase to produce significant deposits (Stelling et al., 2002). The deposit was thick (>1 m) and continuous in the area sampled. Clast sizes range from fine ash to coarse lapilli, with rare blocks and bombs. The sample is basaltic (50 wt.% SiO_2) in its whole rock and matrix glass composition (Tables C.3, C.4). Plagioclase feldspar is moderately abundant (∼20% modal abundance) and lesser, subequal portions of olivine and clinopyroxene are present (∼3% each). Loose olivine (0.5–1 mm) from ash size fraction is studied. It is typically subhedral–euhedral with occasional dissolution textures. Olivine-hosted melt inclusions occur infrequently and vary in size (40–180 μm, average 70 μm, diameter). Most lack co-entrapped